Supplements

S1 Data quality

S1.1 Discharge and water level data

At the gauging stations, the reliability of the discharge series was assessed by back-analysing the rating curve. As both the water levels and discharge series are available, the rating curves can be recalculated for each series (method 1). In addition, the rating curve has been estimated based on the water level data and cross-section data (see supplement B) using the Strickler equation: $Q = k * i^{\frac{1}{2}} * A * R^{\frac{2}{3}}$, where k is the roughness, i the slope, A the cross-sectional area and R the hydraulic radius (method 2). Hence, two methods where applied to derive the rating curve:

- Method 1: Rating curve recalculated from the recorded water level and discharge time series
- Method 2: Rating curve estimated with the recorded water level data and cross-section data using the Strickler equation. The roughness was calibrated.

This analysis showed that the two methods did not correspond at Bomet, in the Nyangores (Figure S2). At Kapkimolwa, in the Amala, the rating curve changed multiple times, however the results of both methods were similar for high flows. At Mines, the discharge data formed a cloud around the cross-section based estimated discharge. In addition, a sensitivity analysis showed that changes in the cross-section, river width and bank slope, were negligible compared to the anomalies observed between both methods. In addition, the velocity at Mines was calculated based on the entire recorded discharge and water level data and the cross-section data; this maximum velocity was below 1 m/s Figure S1, whereas a velocity of 2.13 m/s and discharge of 529.3 m^3/s was measured in the field in 2012 (GLOWS-FIU, 2012). Therefore, at all three stations, there are significant uncertainties in the rating curve and therefore the discharge data as well. Figure S2 also presents the geometric rating curve based on the hydrological model.

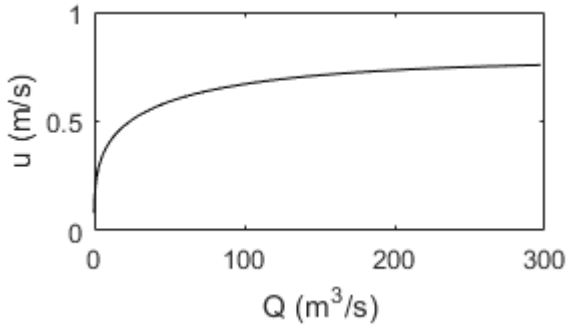

Figure S1: Cross-section average flow velocity – discharge graph at Mines for the entire time period available (1970-2012). This velocity was calculated based on the recorded discharge, water depth and cross-section data

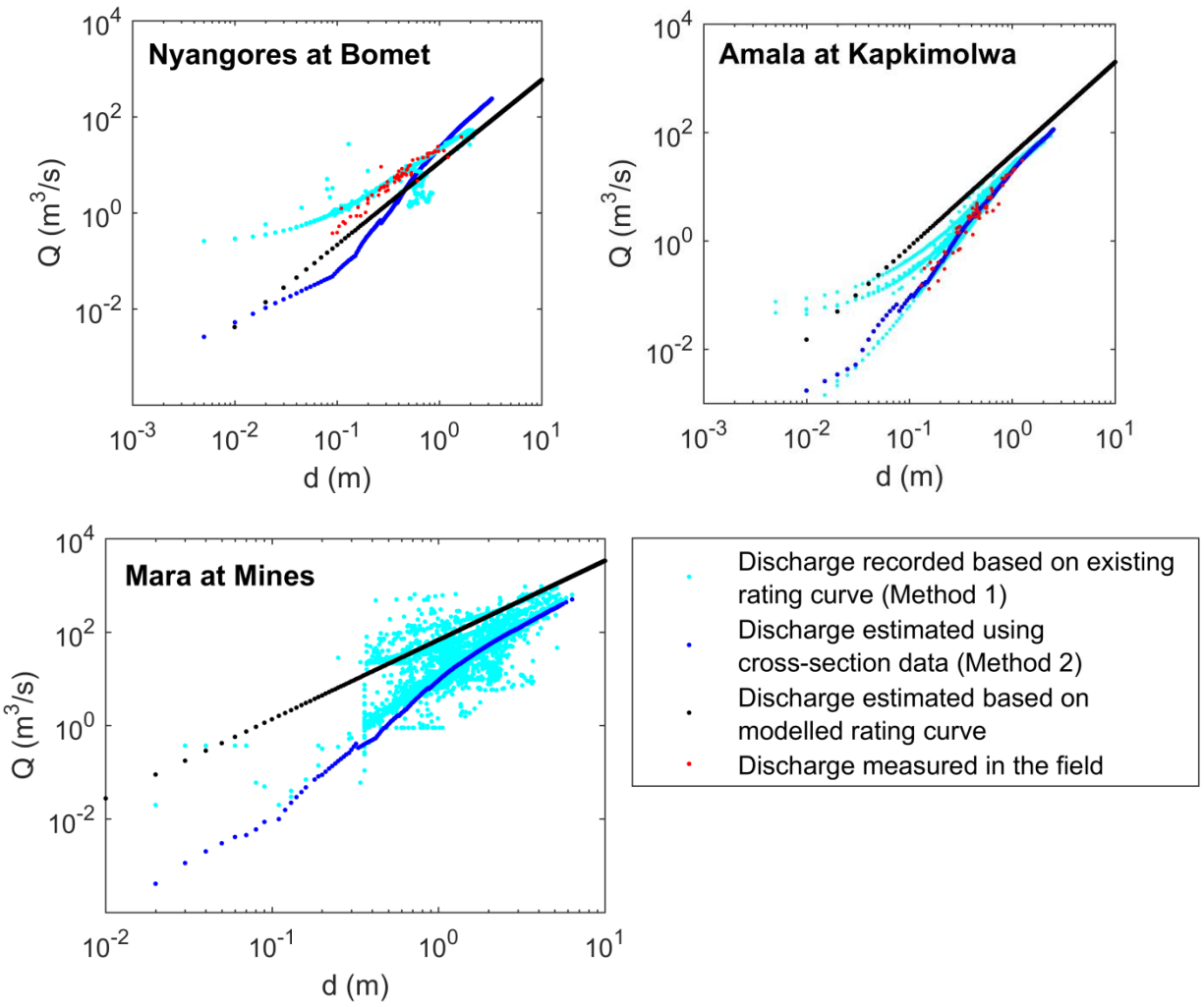

Figure S2: Discharge - water depth graphs for the three main river gauging stations in the Mara River Basin. 1) Recorded discharge and water level time series between 1960 and 2010 (light blue), 2) discharge estimations based on the cross-section (dark blue), 3) discharge calculated with the geometric rating curve based on the hydrological model results for the time period 1970 - 1980 (Nyangores), 1991 - 1992 (Amala) and 1970 - 1974 (Mines), see section on model results (black) and 4) discharge field measurements from the Nile Decision Support Tool (NDST) for the time period 1963 - 1989 (Nyangores) and 1965 - 1992 (Amala), no data was available for Mines (red)

S1.2 Precipitation data

To assess the quality of the data, a double mass curve analysis was done. With this analysis, the cumulative annual rainfall of a station was plotted against the average annual cumulative rainfall of all stations. This curve should be approximately a straight line otherwise the station data is inconsistent and unreliable. As a result of this analysis, inconsistencies were found in 11 out of the 28 stations.

A network analysis was done to assess the spatial correlation between the precipitation stations that were consistent with each other based on the double mass curve analysis. On average the spatial correlation between all stations was 0.6, however the spatial correlation varied in space and time depending on the stations (Figure S3) and the time period used. This change in time and space was confirmed by more detailed analyses of the coefficient of variation using simple statistical formulas and Kriging interpolated precipitation maps (Figure S4). As shown in Figure S4, the southern part of the basin which happens to be the dryer part, has the largest uncertainty in the areal representation of the precipitation.

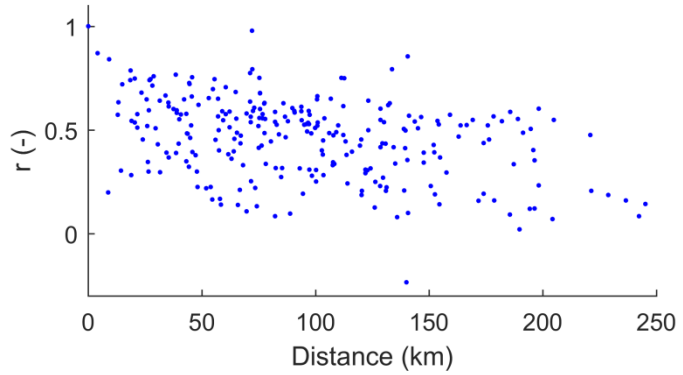

Figure S3: Spatial correlation between all individual precipitation stations plotted against their distance

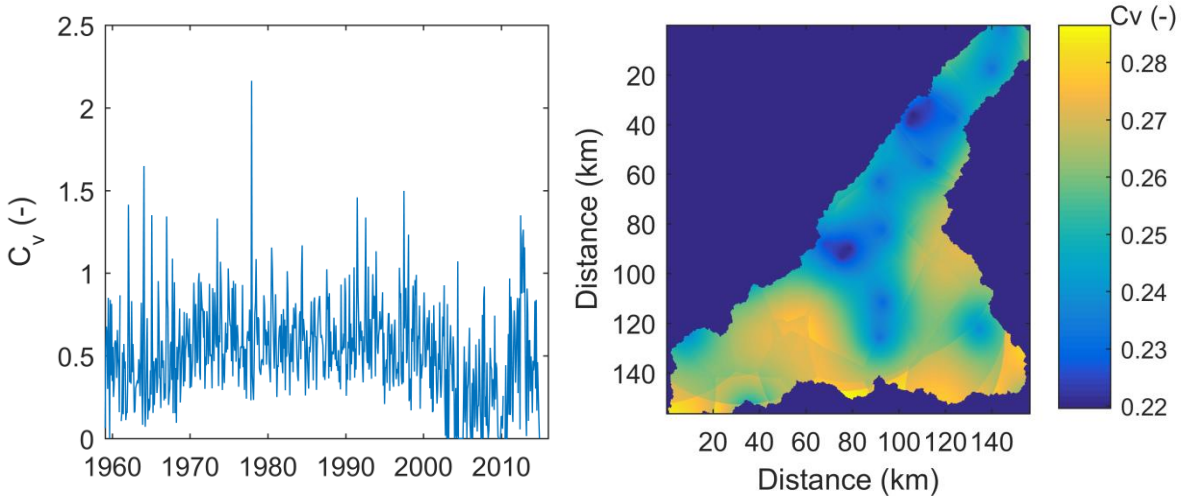

Figure S4: Coefficient of variation C_v of monthly rainfall based on: A) simple statistical formulas and B) Kriging variance of monthly precipitation station data averaged over the time period 1960 - 2010

S2 Effect of parameter and process constraints

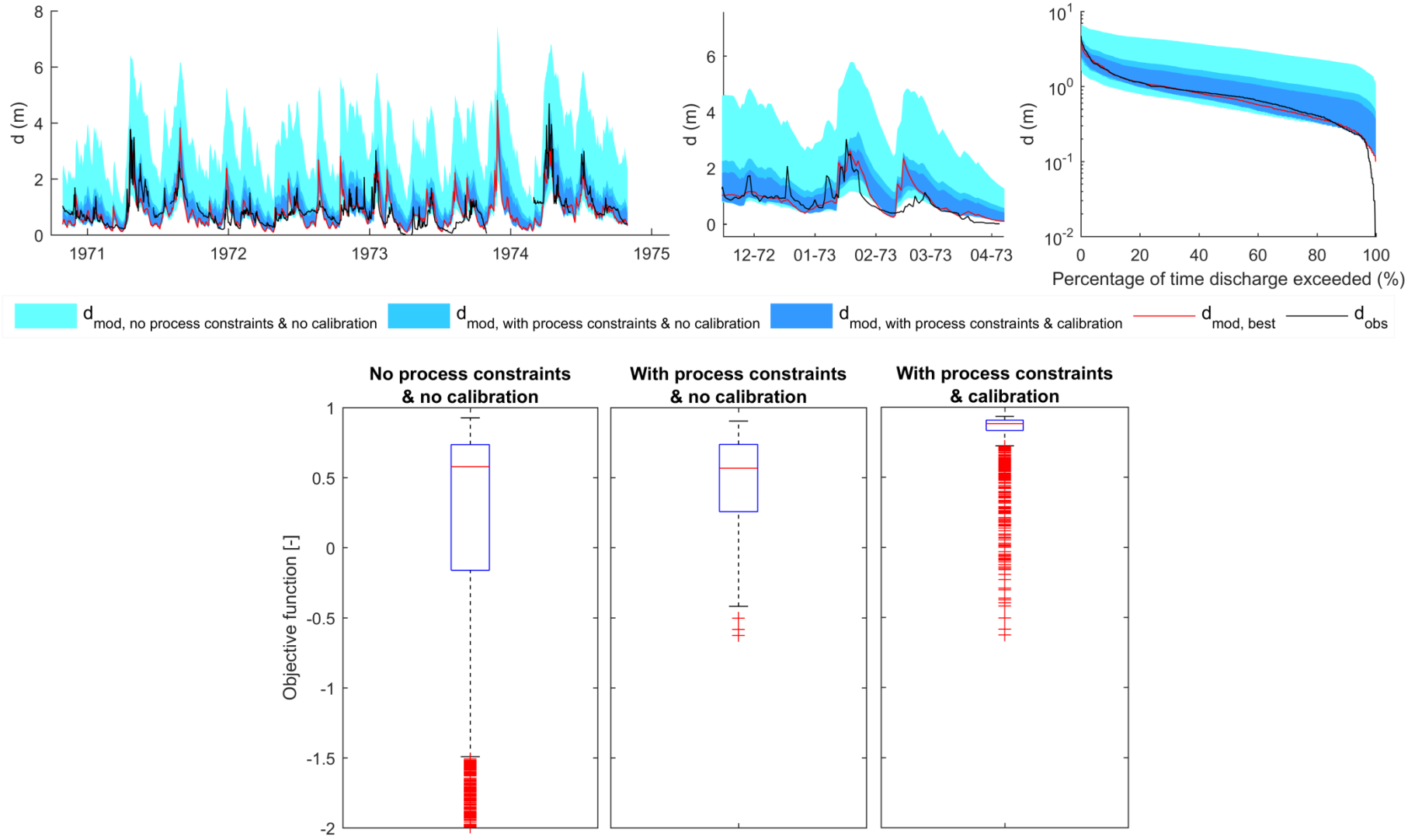

Figure S5: Influence of including process constraints and applying calibration on the modelled water depth using the 5 -/95- percentile as lower/upper limit for the uncertainty range (upper) and on the objective function (lower)

S3 Parameter ranges and values after calibration

Table S1: Values for fixed parameters

Parameters	Parameter value	Unit
K_s	28	d
C_e	0.5	-
S_{umaxF}	122	mm
S_{umaxA}	94	mm
S_{umaxG}	83	mm
S_{umaxS}	89	mm
$S_{max,Amala}$	46	mm
$S_{max,Nyangores}$	74	mm
$S_{max,Middle}$	122	mm
$S_{max,Lemek}$	119	mm
$S_{max,Talek}$	69	mm
$S_{max,Sand}$	29	mm
$S_{max,Lower}$	48	mm

Table S2: Parameter ranges and optimal parameter sets

Parameters	Parameter ranges	Unit	Optimal parameter set		
			Nyangores	Amala	Mines
$I_{max, F}$	0.2 - 2.7	mm	1.26	0.60	2.34
$I_{max, A}$	0.6 - 6.0	mm	1.10	0.60	1.51
$I_{max, G}$	0.7 - 3.6	mm	0.78	0.64	1.56
$I_{max, S}$	0.3 - 2.0	mm	1.24	0.62	1.71
β	0.5 - 2.0	-	1.88	0.62	1.32
T_{lag}	0.5 - 1.5	D	1.45	1.44	1.46
$K_{f,H}$	1 - 28	d	27.24	3.01	6.01
$K_{f,T}$	1 - 28	d	12.02	2.01	3.05
F	0 - 15	mm/d	0.42	12.77	1.71
c	Nyangores : 0.4 - 1.6 Amala : 3.2 - 4.1 Mines : 0 - 2.6	$m^{1/3}/s$	0.89	3.40	1.31
$S_{s,max}$	50 - 150	mm	99.87	106.04	141.98
$S_{F/S}$	0 - 0.5	-	0.27	0.30	0.22
$S_{A/G}$	0 - 0.5	-	0.09	0.33	0.24

S4 Cross-section graphs

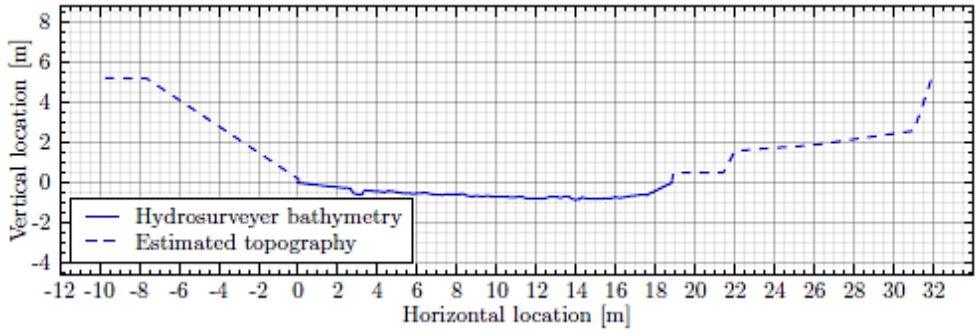

Figure S6: Cross-section at Amala (Rey et al., 2015)

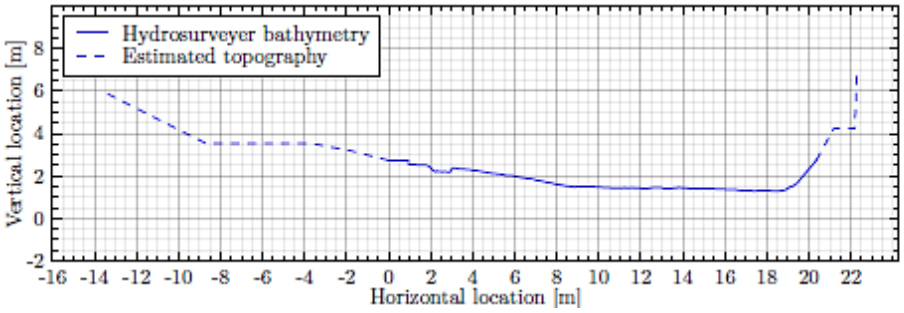

Figure S7: Cross-section at Nyangores Bomet Bridge (Rey et al., 2015)

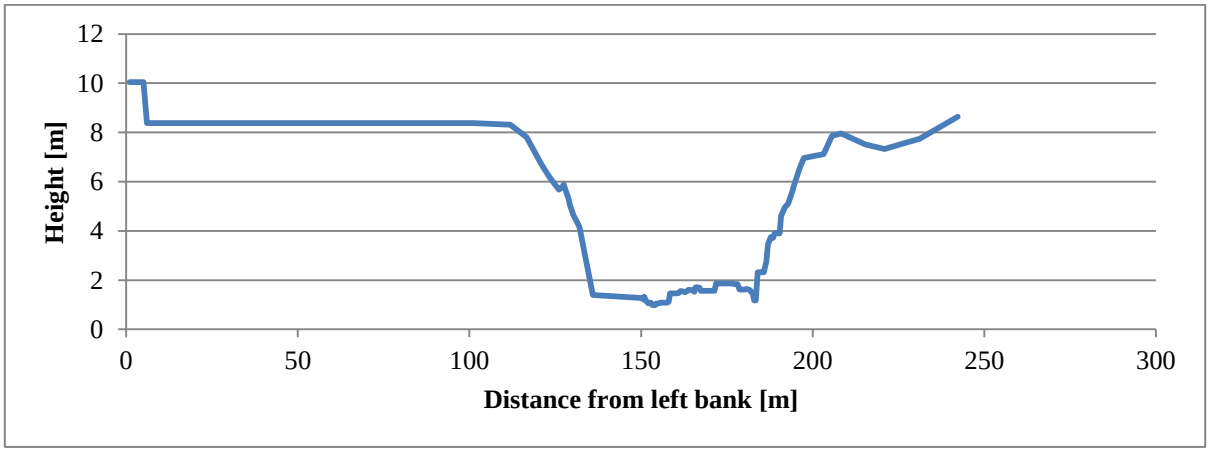

Figure S8: Cross-section at Mara Mines (Stoop, 2017)

S5 Calibration results: discharge time series and duration curves

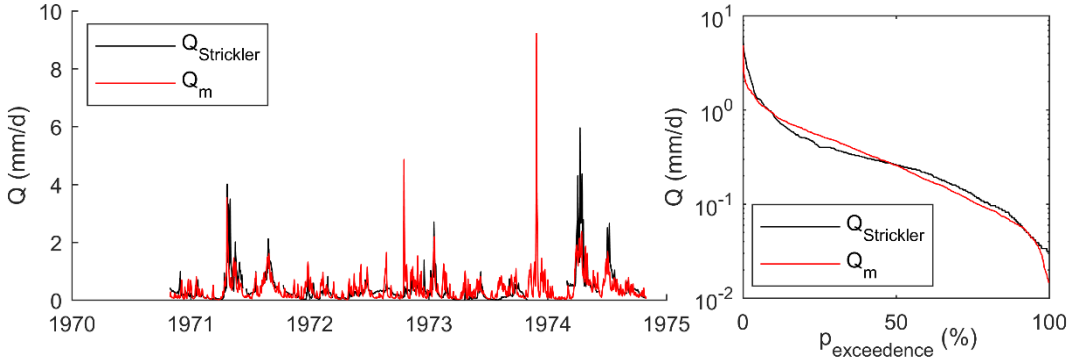

Figure S9: Model results at Mines during calibration: discharge time series and water depth exceedance

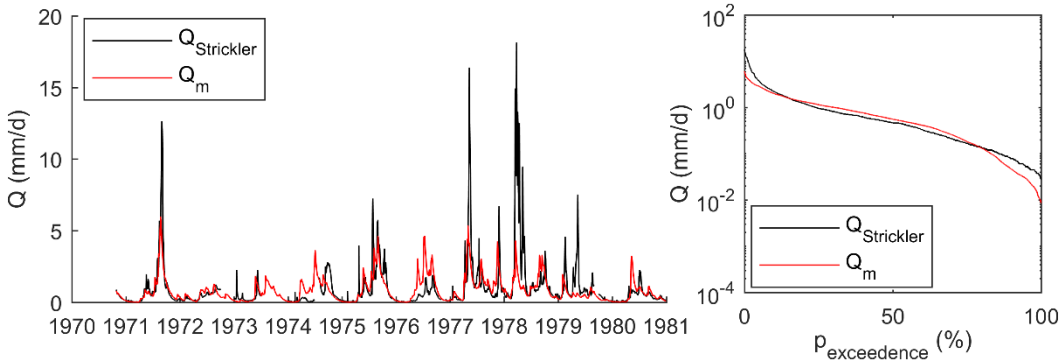

Figure S10: Model results at Nyangores during calibration: discharge time series and water depth exceedance

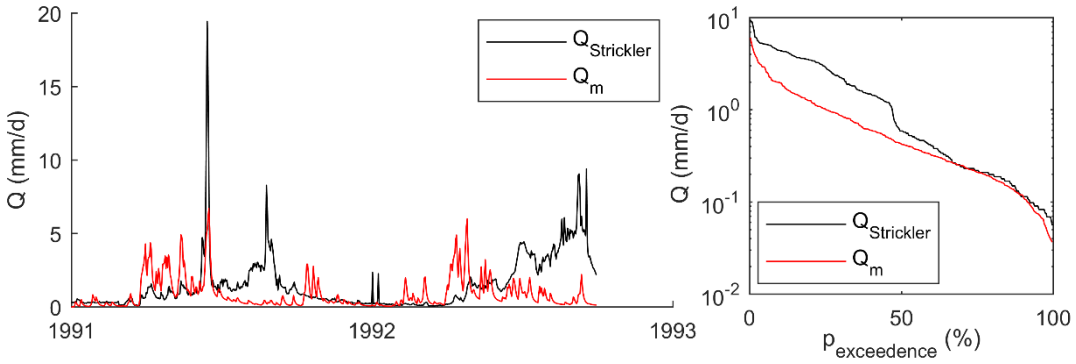

Figure S11: Model results at Amala during calibration: discharge time series and water depth exceedance

S6 Validation results: water level time series and duration curves

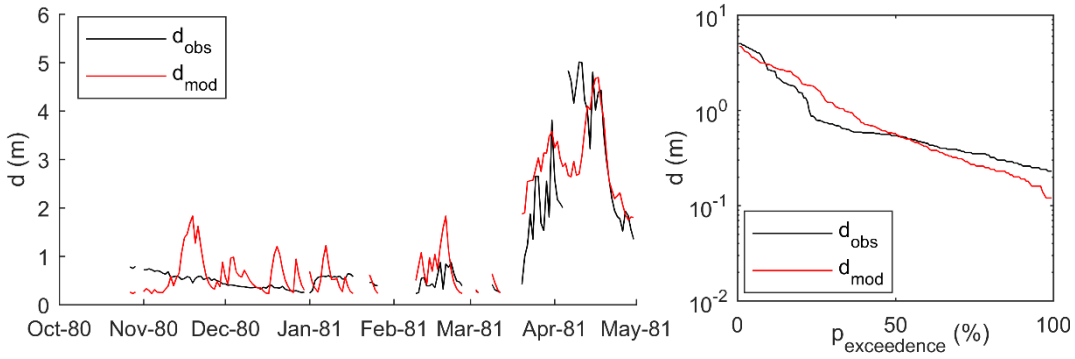

Figure S12: Model results at Mines during validation: water depth time series and water depth exceedance

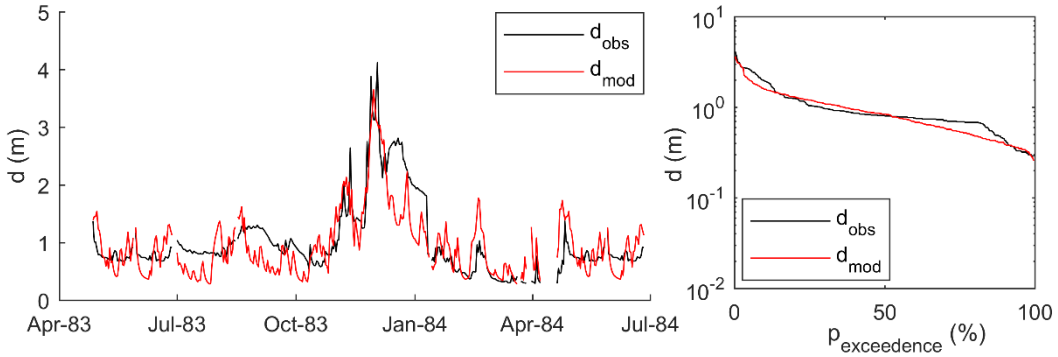

Figure S13: Model results at Mines during validation: water depth time series and water depth exceedance

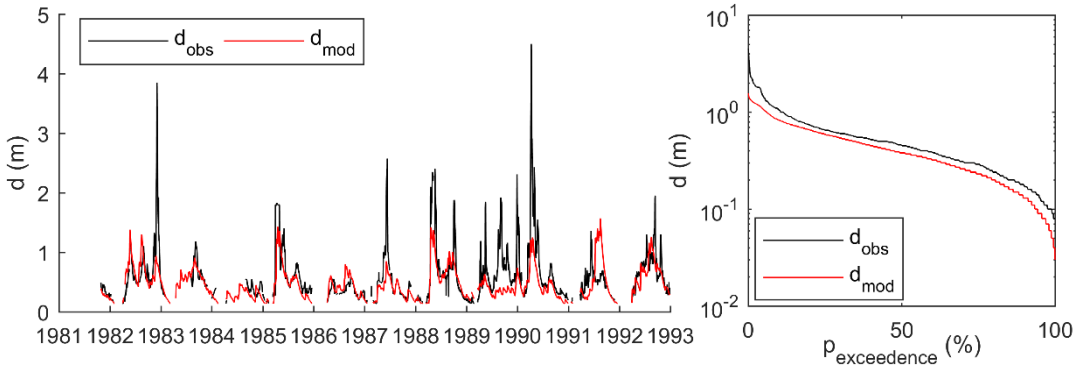

Figure S14: Model results at Nyangores during validation: water depth time series and water depth exceedance

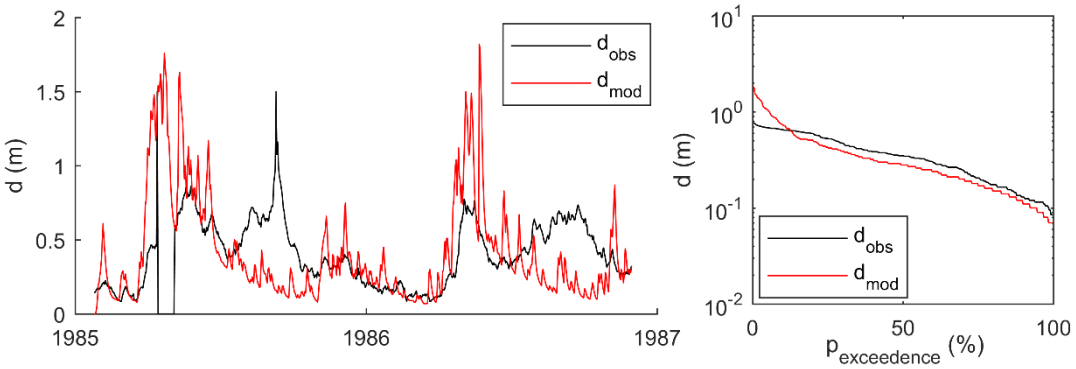

Figure S15: Model results at Amala during validation: water depth time series and water depth exceedance

S7 Validation results: discharge time series and duration curves

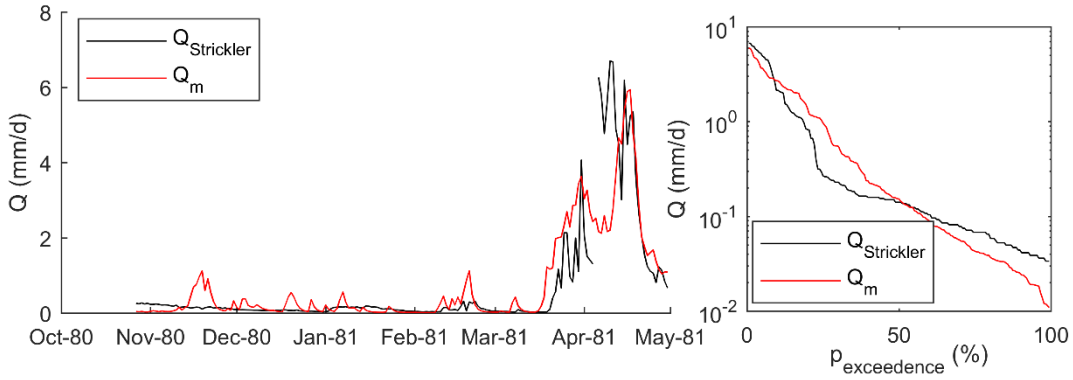

Figure S16: Model results at Mines during validation: discharge time series and water depth exceedance

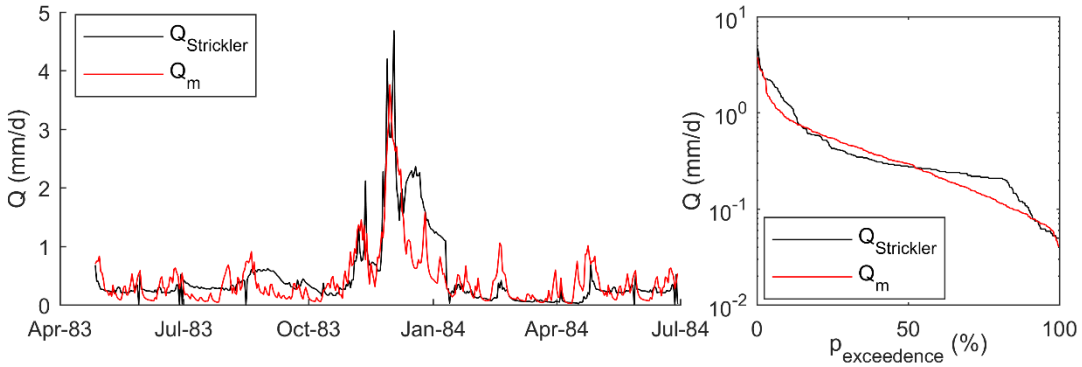

Figure S17: Model results at Mines during validation: discharge time series and water depth exceedance

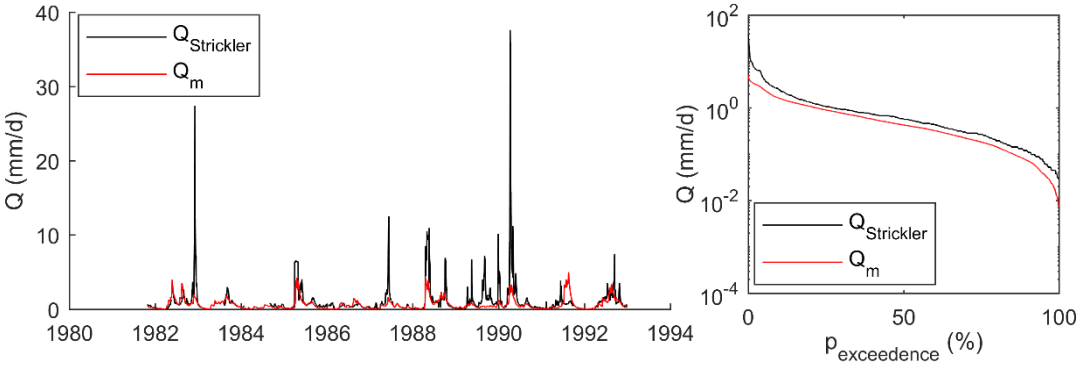

Figure S18: Model results at Nyangores during validation: discharge time series and water depth exceedance

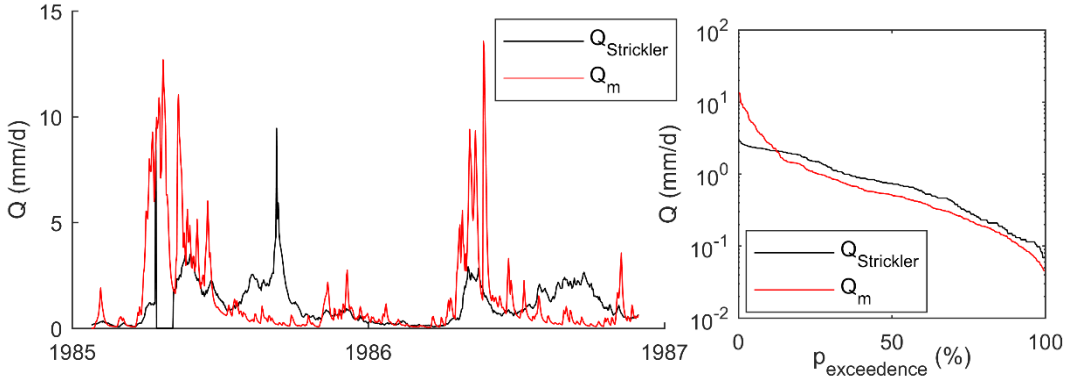

Figure S19: Model results at Amala during validation: discharge time series and water depth exceedance